

# Characterization of a $\gamma$ -adaptin ear-binding motif in enthoprotin

Sylwia Wasiak<sup>a</sup>, Alexei Yu. Denisov<sup>b</sup>, Zhaozhong Han<sup>c</sup>, Peter A. Leventis<sup>d</sup>,  
Elaine de Heuvel<sup>a</sup>, Gabrielle L. Boulianne<sup>d</sup>, Brian K. Kay<sup>c</sup>, Kalle Gehring<sup>b</sup>,  
Peter S. McPherson<sup>a,\*</sup>

<sup>a</sup>Department of Neurology and Neurosurgery, Montreal Neurological Institute, McGill University, 3801 University St., Montreal, QC, Canada H3A 2B4

<sup>b</sup>Department of Biochemistry and Montreal Joint Centre for Structural Biology, McGill University, Montreal, QC, Canada H3G 1Y6

<sup>c</sup>Biosciences Division, Argonne National Laboratories, Argonne, IL 60439, USA

<sup>d</sup>Department of Molecular and Medical Genetics, Developmental Biology Program, Hospital for Sick Children, University of Toronto, Toronto, ON, Canada M5G 1X8

Received 24 September 2003; revised 24 October 2003; accepted 26 October 2003

First published online 18 November 2003

Edited by Felix Wieland

**Abstract** Enthoprotin, a newly identified component of clathrin-coated vesicles, interacts with the *trans*-Golgi network (TGN) clathrin adapters AP-1 and GGA2. Here we perform a multi-faceted analysis of the site in enthoprotin that is responsible for the binding to the  $\gamma$ -adaptin ear ( $\gamma$ -ear) domain of AP-1. Alanine scan mutagenesis and nuclear magnetic resonance (NMR) studies reveal the full extent of the site as well as critical residues for this interaction. NMR studies of the  $\gamma$ -ear in complex with a synthetic peptide from enthoprotin provide structural details of the binding site for TGN accessory proteins within the  $\gamma$ -ear.

© 2003 Federation of European Biochemical Societies. Published by Elsevier B.V. All rights reserved.

**Key words:** AP-1; AP-2; Clathrin; Clathrin-coated vesicle; NMR, *trans*-Golgi network

## 1. Introduction

Internalization via clathrin-coated pits and clathrin-coated vesicles (CCVs) constitutes the major route of endocytic entry into cells [1]. Central to this process is the clathrin adapter protein 2 (AP-2), a heterotetramer composed of  $\alpha$ -,  $\beta$ 2-,  $\mu$ 2-, and  $\sigma$ 2-adaptins [2]. At the *trans*-Golgi network (TGN), CCVs mediate the transport of cargo proteins from the secretory pathway to the endosomal/lysosomal system [3]. This event is regulated by the heterotetrameric AP-1 complex, composed of  $\gamma$ -,  $\beta$ 1-,  $\mu$ 1-, and  $\sigma$ 1-adaptins [4]. A family of monomeric clathrin adapters that are functionally related to AP-1 and AP-2, the Golgi-localized,  $\gamma$ -ear-containing, Arf-binding proteins (GGA1–3), have also been described at the TGN/endosome [5,6].

At their C-termini,  $\beta$ -,  $\alpha$ -,  $\gamma$ -adaptins and GGAs contain globular structures termed ‘ear’ domains. The structure of the  $\alpha$ -ear has been determined at 1.4 Å resolution and is composed of a proximal  $\beta$ -sandwich domain and a distal mixed  $\alpha$ - $\beta$  platform domain [7,8]. The  $\alpha$ -ear serves as a protein scaffold that allows AP-2 to recruit a diverse array of endocytic accessory proteins to sites of CCV formation

[9,10]. These proteins bind to the  $\alpha$ -ear through three short yet distinct consensus peptide motifs, DPF/W, FXDXF, and WVQF [7,8,11,12]. The structures of the  $\gamma$ -ear and the GGA ear (GAE domain) have also been solved [13,14]. These domains have nearly identical folds and are structurally conserved with the  $\beta$ -sandwich domain of the  $\alpha$ -ear [13–15]. Analogous to the  $\alpha$ -ear, the  $\gamma$ -ear and the GAE domain function to recruit accessory proteins to clathrin bud sites [3]. However, the subset of accessory proteins that interact with the  $\gamma$ -ear and the GAE domain at the TGN and endosome, and the peptide motifs mediating these interactions, are distinct from those observed for the  $\alpha$ -ear [3].

Using a proteomic analysis of CCVs, we recently identified enthoprotin, a novel AP-1- and GGA2-binding partner [16]. Enthoprotin was independently identified and termed Clint [17] and epsinR [18,19]. At its N-terminus, enthoprotin contains an epsin N-terminal homology (ENTH) domain. The ENTH domain mediates interactions with phospholipids and proteins and is found primarily in proteins that function in clathrin-mediated endocytosis [20,21]. However, enthoprotin is unique among known ENTH domain-containing proteins in mammals in that it functions in clathrin-mediated budding at the TGN [16–19].

The binding of enthoprotin to AP-1 and GGA2 is mediated via the  $\gamma$ -ear and the GAE domain, respectively [16–19]. Recently, two sequences of differing affinity have been identified as  $\gamma$ -ear-binding sites within enthoprotin [19]. The high-affinity site (site 2) has also been reported to interact with the GAE domain of GGA3 [22]. However, neither of these sites has been characterized in detail. In this study, we perform a biochemical analysis of enthoprotin site 2 and characterize its interactions with the  $\gamma$ -ear. These data provide new insights into enthoprotin/adaptor interactions and an important molecular characterization of the  $\gamma$ -ear/GAE domain-binding motif in enthoprotin.

## 2. Materials and methods

### 2.1. Antibodies and recombinant constructs

Antibodies against the Flag epitope and green fluorescent protein (GFP) were from Sigma and Santa Cruz Biotechnology, respectively. Glutathione *S*-transferase (GST)- $\gamma$ -ear (amino acids 704–822) of mouse  $\gamma$ -adaptin was generated by polymerase chain reaction (PCR) from the I.M.A.G.E. clone 1265666 and was cloned into pGEX-2T (Amersham Biosciences). cDNA KIAA0171 was used as a template

\*Corresponding author. Fax: (1)-514-398 8106.

E-mail address: peter.mcpherson@mcgill.ca (P.S. McPherson).

for PCR to generate Flag-tagged human enthoprotin constructs in pFlag-CMV-2 (Sigma). Deletion mutants lacking amino acids 342–351 (site 1) and 369–378 (site 2) were generated by two rounds of PCR as described [23]. Full-length Flag-tagged enthoprotin and GST-rat epsin ENTH domain were previously described [16,24]. GFP-Eps15 construct was a generous gift of Dr. Pier Paolo Di Fiore (European Institute of Oncology, Milan, Italy).

## 2.2. Alanine scan mutagenesis

To generate alkaline phosphatase (AP)–peptide fusion proteins, double-stranded oligonucleotides encoding wild-type or mutant peptides, corresponding to enthoprotin amino acids 367–379, were cloned into the pEZ707 vector (Z. Han and B.K. Kay, unpublished) at the N-terminus of the mature enzyme. Fusion proteins were expressed in the BL21(DE3) *Escherichia coli* strain. Levels of fusion proteins in crude bacterial extracts were normalized based on AP activity and were serially diluted in Nunc Maxisorp plates (Nalge Nunc International) previously coated with GST- $\gamma$ -ear (200 ng/well) and blocked with 1% bovine serum albumin. The plates were incubated for 1 h at room temperature and then washed with phosphate-buffered saline/0.05% Tween 20. Bound AP fusion proteins were revealed by a colorimetric reaction using paranitrophenyl phosphate.

## 2.3. GST pull-down assays and peptide competition binding assays

Transfected HEK-293 cells were scraped in buffer A (10 mM HEPES-OH, pH 7.4, protease inhibitors) or buffer B (25 mM Tris-HCl, pH 7.4, 150 mM NaCl, 0.5 mM EDTA, protease inhibitors), sonicated and brought to 1% in Triton X-100. Triton X-100-soluble extracts (0.2–1 mg) were incubated for 2 h at 4°C with GST fusion proteins bound to glutathione-Sepharose (Amersham Biosciences). Samples were then washed in appropriate buffer containing 1% Triton

X-100, and specifically bound proteins were processed for Western blot analysis. Peptide competition experiments were performed as described above except that approximately 0.2 nmol of GST fusion protein was pre-incubated with synthetic peptides (synaptojanin 1-ANPFPSLPTRNPFTDRTAAPGNPFR or enthoprotin site 2-NGDFGDWSAF, containing an N-terminal cysteine residue, produced at the Yale University W.M. Keck Facility) prior to addition of cell lysate.

## 2.4. Nuclear magnetic resonance (NMR) spectroscopy

Mouse  $\gamma$ -ear was transferred from pGEX-2T into pGEX-2TK and expressed in *E. coli* BL21 (Gold) strain. Cultures were grown at 37°C in M9 medium supplemented with  $^{15}\text{N}$  ammonium chloride and  $^{13}\text{C}$ -enriched glucose to produce uniformly  $^{15}\text{N}$ - or  $^{15}\text{N}$ ,  $^{13}\text{C}$ -labeled proteins. Following a 6 h induction with 1 mM isopropyl- $\beta$ -D-thiogalactose at 25°C, GST- $\gamma$ -ear was purified and cleaved with thrombin. The NMR samples contained 0.3–1.6 mM protein in buffer C (90%  $\text{H}_2\text{O}$ /10%  $\text{D}_2\text{O}$ , 50 mM sodium phosphate, pH 7.2, 150 mM NaCl, 0.5 mM EDTA and 3 mM dithiothreitol).

NMR spectra were acquired at 30°C on a Bruker DRX-600 spectrometer equipped with triple resonance probes and pulsed field gradients. The following 3D experiments were used for backbone and side chain  $^1\text{H}$ ,  $^{13}\text{C}$  and  $^{15}\text{N}$  resonance assignments: HNCACB, CBCA(CO)HN, HNCO,  $^{15}\text{N}$ -edited NOESY (with mixing time of 90 ms) and  $^{15}\text{N}$ -edited TOCSY [25]. The NMR assignments have been deposited in the BioMagnetic Resonance Bank database under BMRB accession number 5761 ([www.bmrwisc.edu](http://www.bmrwisc.edu)). Detailed analysis of peptide binding to the protein was carried out by comparison of chemical shifts for backbone amide signals in  $^1\text{H}$ - $^{15}\text{N}$  HSQC spectra. HSQC spectra were recorded at 1:4, 1:2, 1:1 and 2:1 peptide to protein ratios that were confirmed by UV concentration of both com-

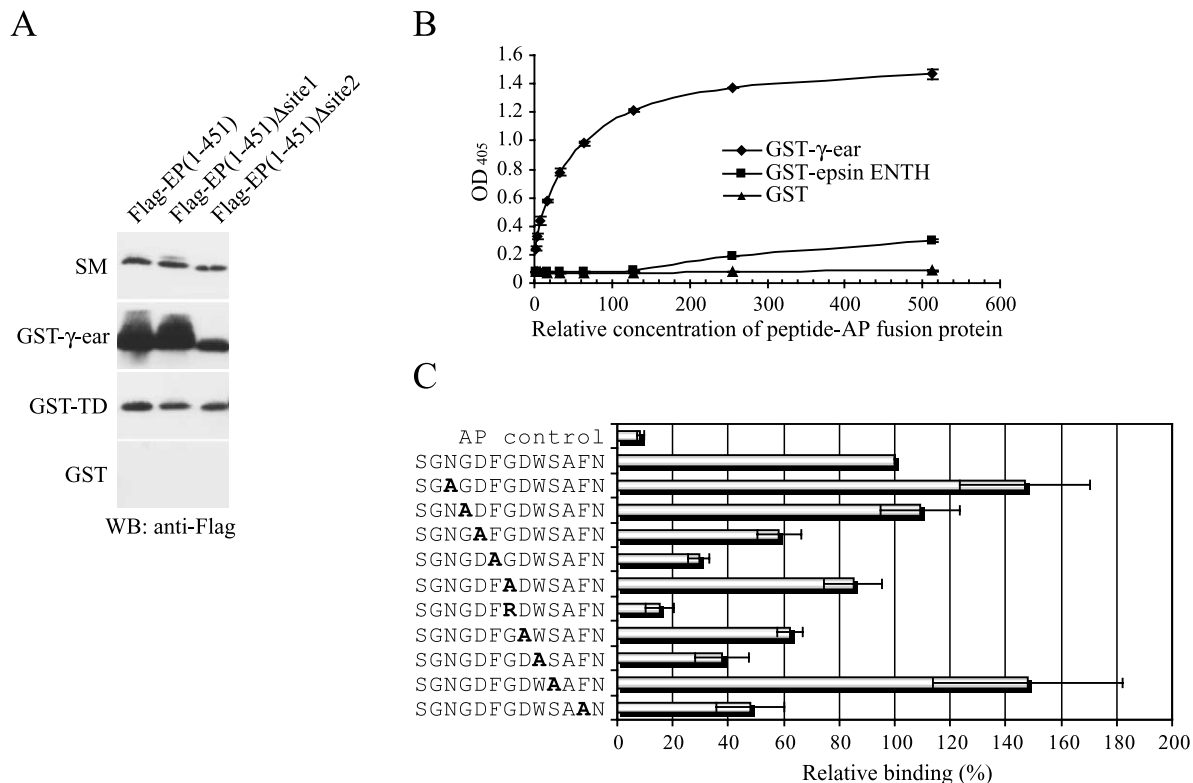


Fig. 1. Mutational analysis of enthoprotin  $\gamma$ -ear-binding site 2. A: Cell lysates containing Flag-tagged enthoprotin (residues 1–451) or residues 1–451 lacking site 1 ( $\Delta$ site 1) or site 2 ( $\Delta$ site 2) were incubated with GST, GST- $\gamma$ -ear, or GST-terminal domain of the clathrin heavy chain (GST-TD) coupled to glutathione-Sepharose. Specifically bound proteins were processed for Western blot (WB) with anti-Flag antibody. An aliquot of the cell lysate (starting material, SM) was processed in parallel. B: A peptide comprising site 2 fused to AP was incubated at increasing concentrations with GST, GST- $\gamma$ -ear, or GST-epsin ENTH domain immobilized on microtiter plates. Specifically bound peptide was detected through AP enzymatic activity, expressed as optical density (OD) at 405 nm wavelength. C: AP fused to peptides with the indicated sequences (mutated amino acids are in bold) was incubated with GST- $\gamma$ -ear immobilized on microtiter plates. Specific binding was detected through AP enzymatic activity and expressed as a percentage of activity seen with the wild-type peptide. Bars represent the mean  $\pm$  S.E.M. of four to six individual experiments performed in triplicate.

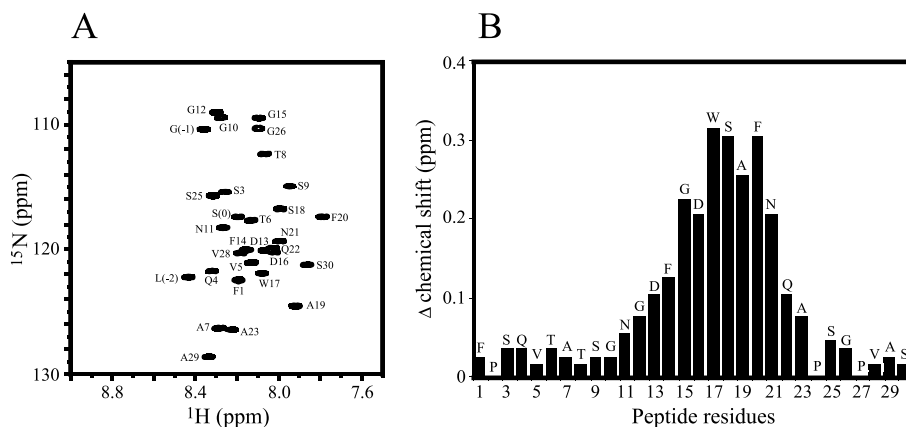


Fig. 2. Mapping of enthoprotin residues involved in binding to the  $\gamma$ -ear. A:  $^{15}\text{N}$ - $^1\text{H}$  HSQC spectrum of the  $^{15}\text{N}$ -labeled 30-amino acid enthoprotin peptide with signal assignments. B: Magnitude of the amide chemical shift changes ( $\{(\Delta^1\text{H shift})^2 + (\Delta^{15}\text{N shift} \times 0.2)^2\}^{1/2}$  in ppm) of the  $^{15}\text{N}$ -labeled 30-amino acid enthoprotin peptide recorded upon binding of the unlabeled  $\gamma$ -ear.

ponents and intensity of He1 (Trp) signals in 1D-NMR. Color figures were generated by the GRASP program [26], and structural data were taken from Protein Data Bank entry IGYU [15].

A sequence encoding residues 359–388 from enthoprotin was subcloned into the pGEX-6P-1 vector and expressed as a  $^{15}\text{N}$ -labeled GST fusion peptide in the *E. coli* BL21 (Gold) strain. For NMR studies, the peptide was cleaved with PreScission Protease (Amersham Biosciences), purified by reverse-phase chromatography on a C-18 column (Vydac), lyophilized, and resuspended in buffer C at pH 6.5. The  $^{15}\text{N}$ -edited NOESY (mixing time of 200 ms) and  $^{15}\text{N}$ -edited TOCSY experiments were used for the assignment of amide signals in the  $^{15}\text{N}$ - $^1\text{H}$  HSQC spectra at 30°C. NMR titrations of the  $^{15}\text{N}$ -labeled peptide by the unlabeled  $\gamma$ -ear protein were performed as described above. Due to strong broadening of some HSQC signals of the peptide in complex with  $\gamma$ -ear (region between S18 and A23), chemical shift changes were measured for a 1:5 protein to peptide ratio and recalculated for a 1:1 complex.

### 3. Results

Synthetic 12-amino acid peptides encoding two putative  $\gamma$ -ear-binding sites in enthoprotin were previously shown to bind with differing affinities to the  $\gamma$ -ear [19]. To demonstrate that these sequences are important in the context of the protein, we generated enthoprotin constructs lacking these sites. Deletion of site 1 (amino acids 344–353) had no noticeable effect on the binding of enthoprotin to  $\gamma$ -ear whereas deletion of site 2 (amino acids 369–378) led to a significant decrease in binding compared to wild-type protein (Fig. 1A). All constructs were equally expressed and bound comparably to a GST fusion protein of the clathrin terminal domain (Fig. 1A). These data confirm that site 2, which matches the high-affinity site described by Mills et al. [19], is the major  $\gamma$ -ear-binding site in enthoprotin.

To examine the contribution to  $\gamma$ -ear interaction of individual amino acids within site 2, we performed an alanine scan analysis. Wild-type or mutant forms of a site 2 peptide were fused to AP and incubated with purified GST- $\gamma$ -ear in microtiter plates. As expected, the wild-type peptide bound in a dose-dependent, saturable manner to the  $\gamma$ -ear but not to GST or a GST-epsin ENTH construct (Fig. 1B). The alanine scan revealed that three of the mutations (N369A, G370A and S376A) had no effect or led to increased binding (Fig. 1C). In contrast, five alanine mutations (D371A, F372A, D374A, W375A, and F378A) significantly reduced binding (Fig. 1C). Mutation of G373 to A only slightly reduced  $\gamma$ -ear binding,

whereas G373R strongly inhibited the interaction (Fig. 1C). These data reveal amino acids within enthoprotin site 2 critical for  $\gamma$ -ear binding.

We next used NMR studies to explore enthoprotin/ $\gamma$ -ear interactions at a structural level. Comparison of  $^1\text{H}$ - $^{15}\text{N}$  HSQC spectra of a  $^{15}\text{N}$ -labeled 30-amino acid enthoprotin peptide encompassing site 2, in the absence or presence of the  $\gamma$ -ear domain, revealed multiple chemical shift changes, indicative of conformational changes in the amino acids caused by  $\gamma$ -ear interactions (Fig. 2 and data not shown). The most significant changes (0.1–0.3 ppm) correspond to

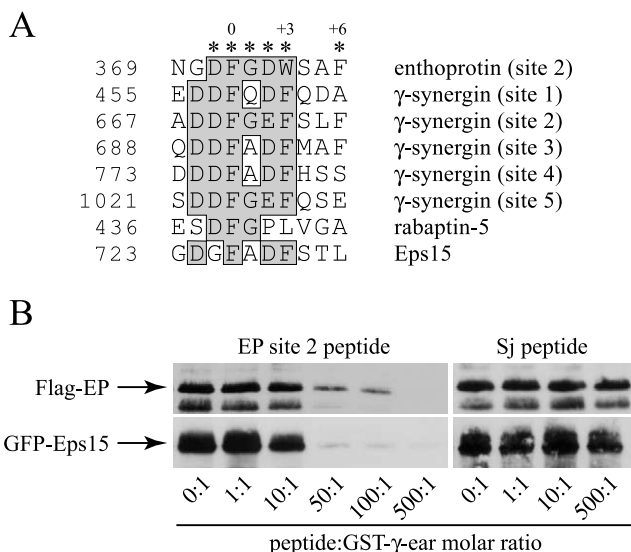


Fig. 3. Eps15 and enthoprotin share an overlapping binding site on the  $\gamma$ -ear. A: Alignment of enthoprotin site 2 with related sequences from various  $\gamma$ -ear-binding proteins. The amino acid number of the first residue is shown. The shading indicates the most frequent amino acids used at any given position and the asterisks denote amino acids in enthoprotin site 2 shown through mutational analysis to decrease binding to  $\gamma$ -ear. B: Lysates from cells transfected with either Flag-tagged full-length enthoprotin (Flag-EP) or GFP-tagged Eps15 were incubated with GST- $\gamma$ -ear fusion protein. A peptide encoding enthoprotin site 2 (EP site 2) or a control peptide from synaptotagmin (Sj) was added to the binding assays at the indicated molar ratios of peptide to fusion protein. Specifically bound proteins were processed for Western blotting with anti-Flag and anti-GFP antibodies.

residues DFGDWSAFNQ (Fig. 2B). This sequence comprises all the amino acids that are critical for  $\gamma$ -ear binding, as mapped by mutagenesis (Fig. 1C). These data reveal the boundaries of the  $\gamma$ -ear-binding site in enthoprotin.

In addition to enthoprotin, a number of mammalian proteins have been shown to bind to the  $\gamma$ -ear including  $\gamma$ -synergisin [27], rabaptin-5 [28], and Eps15 [15]. Each of these proteins contains one or more putative  $\gamma$ -ear/GAE domain-binding sequences related to that in enthoprotin (Fig. 3A). The presence of these sequences suggests that these proteins could occupy the same binding site on the  $\gamma$ -ear and could thus compete with enthoprotin for  $\gamma$ -ear binding. We used Eps15 to test this hypothesis. A peptide encompassing site 2 from enthoprotin (369-NGDFGDWSAF-378) competed the

binding of both Flag-enthoprotin and GFP-Eps15 to GST- $\gamma$ -ear (Fig. 3B). Neither of the proteins was competed by a control peptide from synaptojanin-170 (Sj peptide), encoding three copies of the NPF tripeptide [29] (Fig. 3B). Thus, Eps15 and enthoprotin share an overlapping binding site on the  $\gamma$ -ear. This suggests that, as for binding of endocytic accessory factors to the AP-2  $\alpha$ -ear, multiple components of the budding machinery at the TGN and endosome compete for binding to a shared site on the  $\gamma$ -ear.

The structure of the  $\gamma$ -ear has been recently solved by X-ray crystallography [13,15]. To explore the accessory protein-binding site on the  $\gamma$ -ear at the structural level, we performed a NMR analysis of the  $\gamma$ -ear in the presence of the site 2 peptide from enthoprotin. Comparison of  $^1\text{H}$ - $^{15}\text{N}$  HSQC spectra of

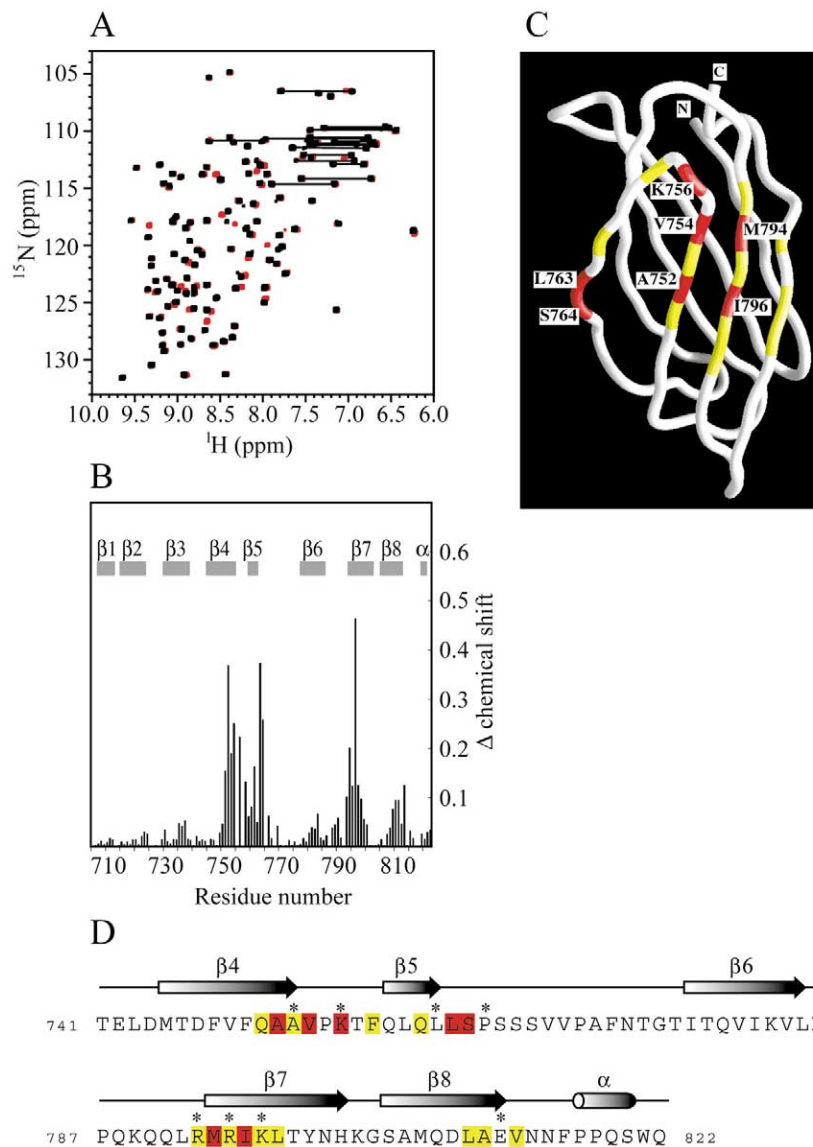


Fig. 4. Structural analysis of  $\gamma$ -ear-binding motif interactions with  $\gamma$ -ear. A: Comparison of  $^1\text{H}$ - $^{15}\text{N}$  HSQC spectra of the  $^{15}\text{N}$ -labeled  $\gamma$ -ear in the absence (black) or presence (red) of the site 2 peptide CNGDFGDWSAF (1:2 peptide to protein ratio). Peaks for two protons of amide groups in Asn and Gln side chains are connected. B: Magnitude of the amide chemical shift changes in ppm of the  $\gamma$ -ear upon binding of the site 2 peptide (1:1 complex). The positions of  $\beta$ -strands are shown. The indicated residue numbers correspond to mouse  $\gamma$ -adaptin. C: The backbone trace of the  $\gamma$ -ear is colored according to the size of the amide chemical shift changes upon binding of the site 2 peptide (red,  $\Delta\delta > 0.1$ ; and white  $\Delta\delta < 0.1$  ppm). Residues showing the largest chemical shift changes are labeled. D: A partial sequence of the mouse  $\gamma$ -ear is shown with  $\beta$ -strands and  $\alpha$ -helices depicted as arrows and rods, respectively. Red and yellow shading represents chemical shift changes as indicated in C. Asterisks mark residues that, when mutated, affect binding to  $\gamma$ -synergisin [13,15].

the  $^{15}\text{N}$ -labeled  $\gamma$ -ear, in the absence or presence of the site 2 peptide, revealed multiple chemical shift changes indicative of conformational changes in the amino acids caused by peptide interactions (Fig. 4A). The magnitudes of the amide chemical shift changes were plotted throughout the length of the  $\gamma$ -ear construct and revealed an effect primarily on residues in  $\beta$ -sheets 4, 5, and 7, with a smaller influence on residues in  $\beta$ -sheet 8 (Fig. 4B). The most extensive shifts were plotted over the crystal structure of the  $\gamma$ -ear revealing a face on the  $\gamma$ -ear, composed of  $\beta$ -sheets 4, 5, 7, and 8, as the binding site for enthoprotin (Fig. 4C).

#### 4. Discussion

A conserved 5–6-amino acid sequence present in several AP-1- and GGA-binding proteins has been identified to mediate the interaction with the  $\gamma$ -ear and the GAE domain (Fig. 3A) [14,19,27,28,30]. Alignment of this sequence has led to the prediction of a consensus  $\gamma$ -ear/GAE domain-binding motif, which is mainly composed of hydrophobic and acidic residues (reviewed in [31]). A strong conservation of the amino acids present at positions  $-1$ ,  $0$ ,  $+2$ , and  $+3$  (Fig. 3A) suggests that these residues may be important for  $\gamma$ -ear interactions. Here, we have systematically tested this prediction. Alanine scan analysis demonstrates that for enthoprotin, D371–W375 form the core of the  $\gamma$ -ear-binding motif. A strong reduction in binding was seen with mutation of the two aromatic residues F372 and W375 to A. F372 in enthoprotin is the only amino acid that is conserved amongst all of the known and putative ear-binding sites (position 0) (Fig. 3A) [31,32]. Although the W is found only in enthoprotin site 2, all other sequences contain a hydrophobic residue at position  $+3$ , with F being the most frequent. Given that W375A showed reduced binding and that the L that occupies this position in rabaptin-5 is also necessary for binding [28], it appears that a bulky hydrophobic residue at position  $+3$  is important for ear domain interactions. Within most sequences, the amino acid that follows the invariant F at position 0 is either G or A (Fig. 3A). This position is occupied by G373 in enthoprotin site 2. G373A slightly decreased  $\gamma$ -ear binding, showing that alanine residues are not optimal, but are tolerated at this position. Mutation of G373 to R strongly reduced binding, suggesting that a small side chain is necessary in this position to be permissive for binding.

A notable observation was that F378A had a strong effect on  $\gamma$ -ear interactions. Moreover, in NMR experiments, F378 was seen to undergo a strong shift change upon binding to the  $\gamma$ -ear. Thus, the F appears to be important for the stability of enthoprotin site 2 interactions with the  $\gamma$ -ear, demonstrating that the  $\gamma$ -ear-binding motif extends C-terminal to the conserved core sequence. The position at  $+6$  has not been predicted to be part of the  $\gamma$ -ear/GAE domain-binding motif [19,31]. Interestingly, co-crystallization of the GGA3-GAE domain with a peptide encompassing the GAE domain-binding site from rabaptin-5 revealed that the alanine residue at position  $+6$  makes contact with residues situated at the end of the  $\beta 5$  strand [22]. In NMR experiments, we observe a strong shift change in the corresponding area of the  $\gamma$ -ear upon enthoprotin peptide binding. Therefore, it is interesting to speculate that variability at position  $+6$  may be one of the determinants that confer specificity to the interactions of different accessory proteins with the  $\gamma$ -ear and the GAE domains.

Two recent studies used X-ray crystallography to determine the structure of the GAE domain of GGA1 and GGA3 in complex with peptides from p56 (DDDDFGGFEEAETFD) and rabaptin-5 (DESDFGPLVGADS), respectively [22,32]. However, no structural data have been available on the interactions of the  $\gamma$ -ear with its ligands. Based on mutational analysis, Kent and colleagues [15] proposed that the ligand-binding site in the  $\gamma$ -ear is composed of a shallow trough formed where  $\beta$ -sheets 4 and 5 meet and they demonstrated that A753 in  $\beta$ -sheet 4, L762 in  $\beta$ -sheet 5 and P765 in the  $\beta 5/\beta 6$  loop, which also lies within the  $\beta 4/\beta 5$  trough, contribute to  $\gamma$ -synergic binding. On the other hand, Nogi and colleagues [13] proposed that ligand binding to  $\gamma$ -ear is mediated by a basic surface comprised of amino acids R793, R795, and K797 in  $\beta$ -sheet 7 and K756 in  $\beta$ -sheet 4. NMR analysis of the  $\gamma$ -ear in complex with the enthoprotin site 2 peptide reveals that the binding site is composed of residues within  $\beta$ -sheets 4, 5, 7, and 8 that align on one face of the  $\gamma$ -ear (Fig. 4C).

In general, the NMR results reported here are consistent with the previous mutational analyses on the  $\gamma$ -ear as well as with the crystallographic analysis of the GAE domains in complex with their ligands [13,15,22,32] (Fig. 4D). Of the seven residues that demonstrate the largest chemical shift changes, four of them, A752, V754, M794 and I796, have their side chains oriented inside the  $\gamma$ -ear  $\beta$ -sandwich (Fig. 4D). However, based on the general geometrical structure of  $\beta$ -sheets, it is reasonable to propose that the observed NMR changes for these backbone amide groups are accounted for by steric contacts with the side chains of preceding amino acids. Thus, Q751, A753, R793, and R795, which each have side chains that are oriented into solution, may interact with the enthoprotin peptide directly (Fig. 4D). Large chemical shift changes were also seen for K756, L763, and S764, which all have side chains in solution that could contribute to ligand binding. Previously, Mills et al. [19] demonstrated that L762 in the  $\gamma$ -ear is necessary for binding to enthoprotin and similarly, we have observed that a GST- $\gamma$ -ear L762E construct fails to bind endogenous enthoprotin (data not shown). The lack of a chemical shift change for L762 in the NMR analysis reported here (Fig. 4D) does not exclude that L762 is contacted by ligand as its chemical shift change could be compensated by a steric contact with the side chain of Q761. Thus, NMR analysis coupled with mutational studies has provided a complementary view of the enthoprotin-binding site within the  $\gamma$ -ear. Detailed analysis of the  $\gamma$ -ear/GAE domain-binding motif sequences in TGN accessory proteins including enthoprotin will lead to a better understanding of the selectivity that underlies the formation of protein networks at the TGN and endosomes.

*Acknowledgements:* We thank the Kazusa DNA Research Institute and Dr. Pier Paolo Di Fiore for DNA constructs used in this study. We would also like to thank Drs. Brigitte Ritter, Annie Angers, and other members of the McPherson laboratory for discussion. Peptides were generated at the Yale University W.M. Keck Facility. This work was generously supported by grants from the Canadian Institutes of Health Research (CIHR) to P.S.M. (MOP62684) and G.L.B. K.G. was supported by a grant from Genome Quebec. Z.Z.H. and B.K.K. are supported by a Laboratory Directed Research Development Award from the Argonne National Laboratory. S.W. and P.A.L. are recipients of CIHR Doctoral Research Awards. P.S.M. and G.L.B. are CIHR Investigators. P.S.M. is a Killam Scholar of

the Montreal Neurological Institute and a McGill University William Dawson Scholar.

## References

- [1] Conner, S.D. and Schmid, S.L. (2003) *Nature* 422, 37–44.
- [2] Brodsky, F.M., Chen, C.Y., Knuehl, C., Towler, M.C. and Wakeham, D.E. (2001) *Annu. Rev. Cell Dev. Biol.* 17, 517–568.
- [3] Hinners, I. and Tooze, S.A. (2003) *J. Cell Sci.* 116, 763–771.
- [4] Traub, L.M. and Kornfeld, S. (1997) *Curr. Opin. Cell Biol.* 9, 527–533.
- [5] Boman, A.L. (2001) *J. Cell Sci.* 114, 3413–3418.
- [6] Robinson, M.S. and Bonifacino, J.S. (2001) *Curr. Opin. Cell Biol.* 13, 444–453.
- [7] Owen, D.J., Vallis, Y., Noble, M.E., Hunter, J.B., Dafforn, T.R., Evans, P.R. and McMahon, H.T. (1999) *Cell* 97, 805–815.
- [8] Traub, L.M., Downs, M.A., Westrich, J.L. and Fremont, D.H. (1999) *Proc. Natl. Acad. Sci. USA* 96, 8907–8912.
- [9] Slepnev, V.I. and de Camilli, P. (2000) *Nat. Rev. Neurosci.* 1, 161–172.
- [10] Takei, K. and Haucke, V. (2001) *Trends Cell Biol.* 11, 385–391.
- [11] Brett, T.J., Traub, L.M. and Fremont, D.H. (2002) *Structure* 10, 797–809.
- [12] Ritter, B., Philie, J., Girard, M., Tung, E., Blondeau, F. and McPherson, P.S. (2003) *EMBO Rep.* 4, 1089–1093.
- [13] Nogi, T., Shiba, Y., Kawasaki, M., Shiba, T., Matsugaki, N., Igarashi, N., Suzuki, M., Kato, R., Takatsu, H., Nakayama, K. and Wakatsuki, S. (2002) *Nat. Struct. Biol.* 9, 527–531.
- [14] Lui, W.W., Collins, B.M., Hirst, J., Motley, A., Millar, C., Schu, P., Owen, D.J. and Robinson, M.S. (2003) *Mol. Biol. Cell* 14, 2385–2398.
- [15] Kent, H.M., McMahon, H.T., Evans, P.R., Benmerah, A. and Owen, D.J. (2002) *Structure* 10, 1139–1148.
- [16] Wasiak, S., Legendre-Guillemin, V., Puertollano, R., Blondeau, F., Girard, M., de Heuvel, E., Boismenu, D., Bell, A.W., Bonifacino, J.S. and McPherson, P.S. (2002) *J. Cell Biol.* 158, 855–862.
- [17] Kalthoff, C., Groos, S., Kohl, R., Mahrhold, S. and Ungewickell, E.J. (2002) *Mol. Biol. Cell* 13, 4060–4073.
- [18] Hirst, J., Motley, A., Harasaki, K., Peak Chew, S.Y. and Robinson, M.S. (2003) *Mol. Biol. Cell* 14, 625–641.
- [19] Mills, I.G., Praefcke, G.J., Vallis, Y., Peter, B.J., Olesen, L.E., Gallop, J.L., Butler, P.J., Evans, P.R. and McMahon, H.T. (2003) *J. Cell Biol.* 160, 213–222.
- [20] De Camilli, P., Chen, H., Hyman, J., Panepucci, E., Bateman, A. and Brunger, A.T. (2002) *FEBS Lett.* 513, 11–18.
- [21] Legendre-Guillemin, V., Wasiak, S., Hussain, N.K., Angers, A. and McPherson, P.S. (2003) *J. Cell Sci.* (in press).
- [22] Miller, G.J., Mattera, R., Bonifacino, J.S. and Hurley, J.H. (2003) *Nat. Struct. Biol.* 10, 599–606.
- [23] Ramjaun, A.R. and McPherson, P.S. (1998) *J. Neurochem.* 70, 2369–2376.
- [24] Hussain, N.K., Yamabhai, M., Bhakar, A.L., Metzler, M., Ferguson, S.S., Hayden, M.R., McPherson, P.S. and Kay, B.K. (2003) *J. Biol. Chem.* 278, 28823–28830.
- [25] Cavanagh, J., Fairbrother, W.J., Palmer, A.G. and Skelton, N.J. (1996) *Protein NMR Spectroscopy: Principles and Practice*, Academic Press, San Diego, CA.
- [26] Nicholls, A., Sharp, K.A. and Honig, B. (1991) *Proteins* 11, 281–296.
- [27] Page, L.J., Sowerby, P.J., Lui, W.W. and Robinson, M.S. (1999) *J. Cell Biol.* 146, 993–1004.
- [28] Mattera, R., Arighi, C.N., Lodge, R., Zerial, M. and Bonifacino, J.S. (2003) *EMBO J.* 22, 78–88.
- [29] McPherson, P.S., de Heuvel, E., Phillie, J., Wang, W., Sengar, A. and Egan, S. (1998) *Biochem. Biophys. Res. Commun.* 244, 701–705.
- [30] Duncan, M.C., Costaguta, G. and Payne, G.S. (2003) *Nat. Cell Biol.* 5, 77–81.
- [31] Duncan, M.C. and Payne, G.S. (2003) *Trends Cell Biol.* 13, 211–215.
- [32] Collins, B.M., Praefcke, G.J., Robinson, M.S. and Owen, D.J. (2003) *Nat. Struct. Biol.* 10, 607–613.